CLM - P 9

CULHAM LABORATORY
LIBRARY
16 JUL 1962

CLM - P 9

United Kingdom Atomic Energy Authority

RESEARCH GROUP

Paper

THE SPECTROSCOPY OF NON-THERMAL PLASMAS

R. WILSON

Culham Laboratory,

Culham, Abingdon, Berkshire

1962

© UNITED KINGDOM ATOMIC ENERGY AUTHORITY - 1962

Enquiries about copyright and reproduction should be addressed to The Librarian, Culham Laboratory, Culham, Abingdon, Berkshire, England.

UNCLASSIFIED
(Approved for Publication)

CLM - P 9

THE SPECTROSCOPY OF NON-THERMAL PLASMAS

by

R. Wilson

A paper read at the 'First International Conference on Vacuum Ultraviolet Radiation Physics'. To be published in the Journal of Quantitative Spectroscopy and Radiative Transfer.

U.K.A.E.A. Research Group,
Culham Laboratory,
Culham,
Nr. Abingdon,
Berks.

May, 1962

C O N T E N T S

	Page
Introduction	1
Electron Energy Distribution	2
Ion Energy Distribution	11
Transient Spectra	13
Partial Containment	14
Conclusion	16
References	17

- - - - - - - -

Table I	18

ABSTRACT

The investigation of plasmas by studying the emitted radiation is not a new subject but has long been the main observational technique of the astrophysicist. However, the recent development of controlled thermonuclear research presents problems to the spectroscopist which are very different from those generally treated by the astrophysicist. These differences can be mainly ascribed to the non-thermal nature of the high temperature laboratory plasma and the aim of this paper is to outline the new problems posed by this type of plasma and to indicate what progress has been made. These problems can be placed into five main groups:-

1. Although there are certain domains (e.g. the continuum) where thermal equilibrium exists to a close approximation, in general the complete distribution of electron populations is non-thermal. Thus local thermodynamic equilibrium is not achieved except for certain transitions (e.g. Bremsstrahlung), and Kirchoff's law, which expresses thermal equilibrium in radiation terms, is invalid. An explanation of the plasma radiation then requires a detailed study of the atomic processes governing ionization and excitation.

2. Although the energy distribution of free electrons may be thermal and represented by a temperature $\underline{T}_e$, this is generally not so for the ions. The average kinetic energy $\underline{W}_i$ of any particular ion is then different from that of the electrons and is a function of its charge $\underline{Z}$ and mass $\underline{M}$ i.e.

$$W_i = f(Z,M) \neq k T_e.$$

The function $f(Z,M)$ can be determined experimentally from Doppler widths of spectral lines and used to infer something of the power spectrum of electric fields accelerating the ions. This in turn depends on the general dynamic behaviour and relaxation properties of the plasma.

3. The life-time of the high temperature laboratory plasma is usually short and the growth and decay of ionization can be observed. This necessitates the use of transient solutions of the basic equations.

4. Perfect confining systems have not yet been realized and plasma can escape or enter the system across the magnetic lines of force. Conservation of atoms within the plasma is therefore invalid and these processes must be considered in explaining the detailed form of the spectrum.

5. The important regions of spectroscopic study are the vacuum ultraviolet and soft X-ray regions. These present strong requirements for experimental development and the determination of fundamental spectroscopic and atomic parameters.

THE SPECTROSCOPY OF NON-THERMAL PLASMAS

1. Introduction

Plasma spectroscopy - the study of radiation emitted by plasmas at frequencies above the plasma frequency - is not a new subject but has been the primary observational tool of the astrophysicist for several decades. However, the growth of controlled thermonuclear research has presented spectroscopic problems which are somewhat different from those generally treated by the astrophysicist. These problems are mainly due to the non-thermal nature of high temperature laboratory plasmas and the purpose of this paper is briefly to review these problems and to indicate what advances have been made in understanding the basic physics involved. To do this it is helpful to draw a comparison between a high temperature laboratory plasma and a thermal plasma as represented by a "normal" stellar atmosphere:-

		"Normal" Stellar Atmosphere	High Temperature Laboratory Plasma
		Thermal	Non-thermal
(1)	Electron energy distribution	Local Thermodynamic Equilibrium all ν	Local Thermodynamic Equilibrium some ν
(2)	Ion energy distribution	$T_i = T_e$	$W_i \neq kT_e$
(3)	Time characteristics	Steady State	Transient
(4)	Conservation of particles	Containment	Partial Containment
(5)	Important region for spectroscopic study	Visible	Vacuum Ultraviolet, Soft X-ray

A non-thermal plasma is defined here as one in which (1) and/or (2) apply i.e. when the electron and/or ion energy distributions (over bound and free levels) depart significantly from thermal distributions.

It is not meant by the above comparison that all laboratory and astronomical plasmas fall into non-thermal and thermal groups respectively. The solar spectrum below λ 1500 Å is a display of non-thermal effects; thermal laboratory plasmas can

be set up at moderate temperatures in high pressure arcs[1] and in high density shock tubes.[2] Hence, in discussing the above points for a high temperature laboratory plasma, much that is said will apply in general to a non-thermal plasma.

The following sections will deal with the physics problems raised by items (1) to (4) inclusive for an optically thin plasma. The instrumental problems involved in making spectroscopic observations in the vacuum ultraviolet and soft X-ray regions will not be discussed since they are outside the scope of this paper.

2. Electron Energy Distributions

The radiation from a plasma in local thermodynamic equilibrium obeys Kirchoff's law at all frequencies -

$$\frac{\varepsilon_\nu}{\kappa_\nu} = B_\nu (T_e), \qquad (1)$$

where ε_ν and κ_ν are the emission and absorption coefficients respectively at frequency ν and $B_\nu(T_e)$ is the Planck function. This law expresses thermal equilibrium in terms of radiation quantities.

The type of non-thermal plasma to be discussed here is one which is optically thin at all frequencies above the plasma frequency but for which the free electrons have a Maxwellian energy distribution (see 2.1) and can be represented by an electron temperature T_e. In this case, the population of any particular state cannot be greater than a "thermal population" i.e. a population given by the Boltzmann and Saha equations, and these are replaced by the inequalities -

$$\frac{n_p}{N} \leq \frac{g_p}{P(T_e)} e^{-\chi_p/kT_e} \qquad (2a)$$

$$\frac{N_{i+1}}{N_i} \leq \left(\frac{2\pi m k}{h^2}\right)^{3/2} \frac{2\, P_{i+1}(T_e)}{P_i(T_e)} \frac{T_e^{3/2}}{n_e} e^{-\chi_i/kT_e} \qquad (2b)$$

where n_p, g_p and χ_p are the population density, statistical weight and excitation potential of state p; N is the total population density of the particular atom or ion and $P(T_e)$ is the partition function -

$$P(T_e) = \sum_p g_p \, e^{-\chi_p/kT_e}$$

In expression (2b) the symbols have the same meaning but are ascribed to successive stages of ionization i and (i + 1); n_e is the number density of free electrons and m, k and h are the electron mass, Boltzmann constant and Planck constant respectively.

When inequalities (2a,b) hold, detailed atomic processes must be considered to determine the electron populations and hence the radiation intensity at all frequencies. In the following sub-sections, the form of the electron energy distributions are discussed for non-thermal plasmas.

2.1 Free Electrons

A non-thermal distribution of energies of free electrons can be caused by three factors. (a) Since we are considering optically thin plasmas, photo-excitation processes are negligible and a detailed balance system is therefore impossible. However, if the electron collision rates populating a group of levels are very much faster than radiative decay rates, then all radiative processes become negligible and a detailed balance exists to a close approximation between collisional processes alone and hence the electrons have a thermal distribution (b). In the methods of heating plasmas, the energy is usually imparted to the electrons in a grossly non-thermal fashion e.g. by an applied electric field. However, if the electron-electron relaxation time is short compared to the energy heating time, a thermal distribution will again exist to a close approximation. (c) Although the conditions may be such that a thermal distribution exists in spite of (a) and (b), the electrons may not be contained within the plasma for a sufficient time to allow thermalization. Thus the relaxation time must be short compared to the electron containment time (or the life-time of the plasma) if a thermal distribution is to be attained.

Thus there are three criteria to be satisfied for the free electrons in a plasma to have a Maxwellian energy distribution -

$$t_{ee} \ll t_{rad}, t_{en}, t_{part}, \tag{3}$$

where t_{ee} is the Spitzer electron-electron relaxation time[3], t_{rad} is the energy decay time for Bremsstrahlung radiation, t_{en} is the energy heating time and t_{part} is the particle containment time.

For a fully ionized hydrogen plasma, the first criterion reduced to

$$\frac{0.3\ T_e^{3/2}}{n_e \ln\Lambda} \ll 1.4 \times 10^{11}\ \frac{T_e^{\frac{1}{2}}}{n_e}$$

$$\text{or} \quad T_e \ll 5 \times 10^{11} \ln\Lambda,$$

where T_e is in ^{o}K and $\ln\Lambda$ is a slowly varying function of n_e and T_e of the order of 10. One would therefore expect this criterion to be satisfied for all feasible temperatures and only the second and thired criteria need be considered in practical conditions. In this paper, we limit the discussion to the case where criteria (3) are satisfied i.e. to the case when the free electrons have a Maxwellian energy distribution represented by temperature T_e.

2.2 Coronal Distribution

We now consider the distribution among bound levels and also the ionization state, taking first the extreme non-thermal case when radiative decay rates for bound-bound and free-bound transitions predominate over collision induced decay rates. This is the situation in the Solar Corona and the relevant equations have been derived by WOOLLEY and ALLEN.[4] The population n_p of the p_{th} bound level relative to n_1 the population of the ground state, is given by

$$\frac{n_p}{n_1} = \frac{n_e S_{1p}}{A_p} \tag{4}$$

where S_{1p} is the collisional excitation function for temperature T_e and A_p is the total Einstein transition probability for level p.

The state of ionization is obtained by neglecting the populations of upper bound levels. It is independent of n_e and given by

$$\frac{N_{i+1}}{N_i} = \frac{S}{\alpha} \qquad (5)$$

where N_i and N_{i+1} are the populations of the ith and $(i+1)$th states of ionization, S is the collisional ionization coefficient for transition $i \rightarrow (i+1)$ and α is the radiative recombination coefficient for transition $(i+1) \rightarrow i$.

2.3 General Non-thermal Distribution

In the region between the thermal and coronal domains, the situation is much more complicated and simple equations do not exist to describe the electron distributions. Essentially the problem is to solve the differential equations describing all rates which populate and depopulate each bound level. Considerable advances have been made in the past year due to the work of McWHIRTER[5], BATES and KINGSTON[6] BATES et al[7], and D'ANGELO[8], who took account of the population of upper bound levels to derive recombination rates.

The physical picture which has emerged is that the thermal equilibrium in the continuum extends down to the upper bound levels of the ion due to the high collisional transition rate between the continuum and upper levels. Since this is imposed on the upper levels by the free electrons, the thermal equilibrium of the bound levels is linked to the continuum and their populations are given by the Saha equation.

There is therefore some level in the ion, which we will call the "thermal limit", above which the distributions approximate to thermal and below which they are approximately coronal. The bound levels above the thermal limit are similar to the continuum in certain respects. Any transitions to low levels, by radiative or collisional decay, is equivalent to recombination since the hole that is left is immediately

populated by a collisional transition from the continuum; similarly, any excitation from low levels to the upper thermal levels is equivalent to ionization. The net rates of recombination and ionization are given by BATES et al[7] in terms of binary coefficients which they call the "collisional-radiative recombination coefficient" and the "collisional-radiative ionization coefficient".

For low electron densities, the thermal limit is very close to the ionization limit and we have coronal distributions. As n_e increases, the thermal limit drops lower and lower until, at sufficiently high densities, it reaches the ground level and all levels have a thermal population i.e. the Boltzmann and Saha equations are valid. This is illustrated by Fig. 1 where the calculations of BATES et al[7] for the ionization ratio n^+/n_o in a hydrogen -like plasma are plotted against n_e for $Z = 1$ and $T_e = 16000^oK$. Also shown, in the form of dashed curves, are the coronal (independent of n_e) and thermal ($\propto n_e^{-1}$) distributions. At densities $< 10^{11}$ cm^{-3}, the distribution is coronal and at densities $> 10^{17}$ cm^{-3}, the distribution is thermal; the curve obeys the inequality (2b). The maximum in the curve is due to the fact that although recombination is the more dominant process at high densities the calculations predict a more rapid increase in the ionization rate in the initial stages as n_e increases beyond the coronal domain. The physical reason why this should be so is not clear.

2.4 Semi-Coronal Distribution

Although the concept of a thermal limit is useful in presenting a physical picture, its value as a means for calculating population distributions has yet to be tested. We will develop equations here in the range where the concept is probably most valid i.e. when the thermal limit is near the ionization limit. This allows the use of hydrogen - type equations for the thermally populated levels.

The difficulty is to determine the thermal limit and we use here a definition due to McWHIRTER[9] that this is the level at which upward and downward transitions are

equally probable. Using the collisional excitation and ionization coefficients derived by BATES et al[7] from the SEATION[10] cross sections for positive ions, the principle quantum number t (non-integral) representing the thermal limit in a hydrogen-like ion of nuclear charge Z, is defined by the expression:-

$$n_e n_t \times 1.4 \times 10^{-5} t^2 Z^{-2} T_e^{-\frac{1}{2}} e^{-\chi_t/kT_e} + n_e n_t \sum_{t+1}^{\infty} 4.8 \times 10^{-5} \frac{t^2 q^2}{q^2 - t^2} f(t,q) Z^{-2} T_e^{-\frac{1}{2}} e^{-\chi_{t,q}/kT_e}$$

(collisional ionization) (collisional excitation)

$$= n_t \sum_{1}^{t-1} A_{t,q} + n_e n_t \sum_{1}^{t-1} 4.8 \times 10^{-5} \frac{t^4}{t^2 - q^2} f(q,t) Z^{-2} T_e^{-\frac{1}{2}},$$

(radiative decay) (collisional de-excitation)

where χ_t is the ionization potential for level t and $f(t,q)$ and $A_{t,q}$ are the oscillator strength and Einstein transition probability for the transition $t \rightarrow q$. Since t is large, we can put the exponentials ~ 1 and use asymptotic expressions[11] for f and A. With approximate evaluations of the summations, this gives

$$t^7 = 1.4 \times 10^{15} Z^6 T^{\frac{1}{2}} n_e \qquad (6)$$

We can now transfer to a general ion by making the approximate substitutions $t^2 = \chi_i / \chi_t$ and $Z^2 = \chi_i / \chi_H$ where χ_i and χ_H are the ionization potentials of the ion and hydrogen respectively. This gives

$$\chi_t^7 = 3 \times 10^{-28} \chi_i (kT_e)^{-1} n_e^2 \qquad (7)$$

where χ_i and kT_e are in eV, and n_e in cm^{-3}.

Since the discussion is limited to the case $\chi_t \ll \chi_i$, the situation is similar to the coronal case. Hence the populations of bound levels intermediate between the ground level and thermal limit can be neglected and only the processes of radiative decay from thermal levels and collisional excitation into thermal levels need be considered as contributing to recombination and ionization. Defining the rates of these processes in terms of the binary coefficients α_t and S_t, the ionization ratio is now given by an equation similar to (5) i.e.

$$\frac{N_{i+1}}{N_i} = \frac{S + S_t}{\alpha + \alpha_t} \qquad (8)$$

α_t is given by

$$\alpha_t = \sum_{p=t}^{\infty} \sum_{q=1}^{t-1} N_i^{-1} n_e^{-1} n_p A_{p,q}$$

where n_p, the population density in state p is given by the Saha equation. Using similar approximations as above, this reduces to

$$\alpha_t = 4.2 \times 10^{-6} Z^4 T_e^{-3/2} t^{-2} \qquad (9)$$

For a general ion,

$$\alpha_t = 1.8 \times 10^{-14} \chi_i (kT_e)^{-3/2} \chi_t \qquad (10)$$

S_t is given by

$$S_t = \sum_{t}^{\infty} 4.8 \times 10^{-5} p^2(p^2-1)^{-1} f(1,p) Z^{-2} T_e^{-\frac{1}{2}} e^{-\chi_1 p/kT_e}$$

which approximately reduces to

$$S_t = 3.8 \times 10^{-5} Z^{-2} T_e^{-\frac{1}{2}} t^{-2} e^{-\chi_i/kT_e} \qquad (11)$$

For a general ion,

$$S_t = 4.8 \times 10^{-6} \chi_t \chi_i^{-2} (kT_e)^{-\frac{1}{2}} e^{-\chi_i/kT_e} \qquad (12)$$

2.5 Domains of Validity

We will now establish the domains of n_e and T_e for which the various types of distribution discussed above are valid. A thermal distribution exists among all levels when the thermal limit extends down to the ground state i.e. when $\chi_t = \chi_i$ in equation (7). Since this equation was derived using approximations based on $\chi_t \ll \chi_i$, this hardly seems a valid procedure but it gives essentially the same result as obtained from the criterion that the radiative decay rate from the second to first level of a hydrogen-like ion should be much less (say 10 per cent) than the collisional decay rate i.e.

Thermal Domain: $\quad n_e \geq 6 \times 10^{13} \chi_i^3 (kT_e)^{\frac{1}{2}} \qquad (13)$

In this domain, the Saha and Boltzmann equations describe the distributions.

The coronal domain can be defined by the condition that the rate coefficients α_t, and S_t for the thermal levels should be much less (say 10 per cent) than the corresponding coefficients α and S for the continuum. This gives

Coronal Domain: $n_e \leqslant 1.5 \times 10^{10} \chi_i^{-\frac{1}{2}} (kT_e)^4$ (14)

In this domain, the coronal equations (4) and (5) apply.

To establish the domain where the semi-coronal equations are valid, a comparison was made with the detailed calculations of BATES et al[7] for hydrogen-like ions. This showed an agreement of better than 50 per cent in the net rates of recombination and ionization for -

Semi-Coronal Domain: $n_e \leqslant 10^{11} \chi_i^{3/2} (kT_e)^2$ (15)

The domains defined by equations (13), (14) and (15) are shown in Fig. 2 for the case χ_i = 100 eV, a typical value for ions observed in high temperature plasmas. The range of temperature (1-100 eV) plotted is more than adequate to cover the range where 100 eV ions could be appreciably populated. It would appear that most high temperature laboratory plasmas will fall in the coronal or semi-coronal domains.

In addition to criteria (13), (14) and (15), we have the extra condition that the plasma be optically thin at all frequencies above the plasma frequency for the above distributions to be valid i.e.

$$\tau_\nu \leqslant 0.1 \quad \text{for} \quad \nu > \nu_p \tag{16}$$

where τ_ν is the optical depth at frequency ν and ν_p is the plasma frequency. τ_ν varies considerably with ν and we now evaluate criterion (16) for the three types of photo-absorption (a) bound-bound (b) bound-free (c) free-free transitions, and for electron scattering (d). A spatially uniform plasma model of dimension D is used.

(a) The most serious bound-bound transition is resonance line absorption. For a Doppler broadened profile, the application of (16) to the central frequency gives

$$DN_i \leqslant 7 \Delta\nu_D / f \tag{17}$$

where the population density of the ground state is given approximately by the number density N_i of the absorbing ion or atom, and where $\Delta\nu_D$ is the Doppler frequency width and f the oscillator strength of the line.

(b) The maximum optical depth for photo-ionization is that corresponding to a

transition from the ground state to the absorption edge i.e. $h\nu = \chi_i$. At this frequency, Elwert's[12] adaption of the Kramers absorption coefficient for a general ion gives

$$DN_i \leq 10^{16} \chi_i g p \varepsilon^{-1}, \tag{18}$$

where g is the Gaunt factor, p the quantum number of the ground state and ε the number of optical electrons. The generalised Elwert absorption coefficient for any ion is necessarily rough, but is justified for the present purpose as is adopting the value $g \sim 0.8$.

(c) Using the free-free absorption coefficient,[3] criterion (16) reduces to

$$D n_e^2 \leq 4 \times 10^{37} (kT_e)^{\frac{1}{2}} (h\nu)^3 Z^{-1}, \tag{19}$$

where kT_e and $h\nu$ are in eV and Z is the average charge of the ions in the plasma. This criterion is best evaluated for the region of maximum Bremsstrahlung emission i.e. $h\nu \sim kT_e$.

(d) For electron scattering to produce no appreciable optical depth, the Thompson cross-section gives

$$Dn_e \leq 1.5 \times 10^{24} \tag{20}$$

The relative importance of these optical depth criteria are best illustrated by a numerical example for the case $kT_e = kT_i = 100$eV and D = 100cm. A hydrogen plasma with small quantities of trace elements is considered and (17) and (18) are evaluated for the Ne VIII ion whose resonance line is at 770.4 A^o. The conditions under (a) to (d) then reduce to

(a) $N_i \leq 2 \times 10^{11}$ cm^{-3}

(b) $N_i \leq 4 \times 10^{16}$ cm^{-3}

(c) $n_e \leq 2 \times 10^{21}$ cm^{-3}

(d) $n_e \leq 1.5 \times 10^{22}$ cm^{-3}

It is apparent that criteria (19) and (20) will be easily satisfied in high temperature laboratory plasmas. The most stringent criterion is (18) which places a limit

on the number density of unstripped ions being observed. In the numerical example quoted, about ten per cent of the Ne ions are in stage VIII for a steady state coronal distribution.

If the optical depth criteria are violated, then the electron energy distributions discussed above become invalid. Consider a plasma for which a coronal distribution (criterion (14)) applies; if we increase the dimensions until the optical depth, and hence photo-excitation processes, become large, then a thermal distribution will be imposed on the system but this will develop upwards from the ground level of the ion and not downwards from the continuum as in the case of increasing density. In this case the form of the electron population distributions is a problem of radiative transfer in a non-thermal plasma. The problem is complicated by the fact that the source function $\varepsilon_\nu/\kappa_\nu$ is a function of the optical depth and geometry of the plasma as well as its density and temperature.

3. Ion Energy Distribution

A non-thermal distribution of ion energies raises quite different points of physics than a non-thermal electron distribution. Whereas the latter depend on detailed atomic processes, the former can reflect macroscopic effects and the dynamic behaviour of plasmas. A general approach has been indicated by THONEMANN[13] who set up an equation of motion for ions in the electric field system of a magnetic plasma -

$$\frac{d\bar{v}}{dt} = \frac{Zq}{M}\left[E(\omega,t) + \bar{v} \times \bar{B}\right] - \beta\,\bar{v} \qquad (21)$$

where $\bar{v}$ is the velocity and Zq and M are the charge and mass of the ion; $E(\omega,t)$ is the power spectrum of the electric fields, $\bar{B}$ the magnetic field and β the collision frequency. Collisions are introduced as a "dynamical friction" and hence no account is taken of changes in direction or any relaxation tendency towards a thermal distribution.

In principle, equation (21) can be solved if $E(\omega,t)$ is known, and the average kinetic energy of W_i of each ion expressed terms of its charge and mass -

$$W_i = f(Z,M) , \tag{22}$$

a function which can be determined experimentally from measurements of the Doppler widths of spectral lines and hence used to interpret something of the electric field power spectrum and hence of the plasma behaviour. $E(\omega,t)$ may be due to instabilities in the plasma or a direct result of the mechanism used for heating.

If the plasma is in thermal equilibrium, the power spectrum will have a thermal distribution and W_i is given by

$$W_i = \text{constant} = kT_i \tag{23}$$

Some examples of non-thermal distributions can be given for the simple case when the power spectrum is monochromatic at angular frequency ω and amplitude E_o -

$$\bar{E} \parallel \bar{B}; \qquad \text{all } \omega \qquad W_i = \frac{q^2 E_o^2}{4(\omega^2+\beta^2)} \frac{Z^2}{M} \tag{24}$$

$$\bar{E} \perp \bar{B}; \qquad \omega \gg \omega_c \qquad W_i = \frac{q^2 E_o^2}{4(\omega^2+\beta^2)} \frac{Z^2}{M} \tag{25}$$

$$\bar{E} \perp \bar{B}; \qquad \omega \ll \omega_c \qquad W_i = \frac{\omega_c^2 E_o^2}{4(\omega_c+\beta)^2} M \tag{26}$$

Examples of plasma oscillations which may produce these types of distribution are electron plasma oscillations (24), Whistler mode (25) and Alfèn waves (26).

This general approach has been used by JONES and WILSON[14] to investigate the ion energy distributions in Zeta. Kinetic energies of several ions of trace elements, added in small quantities to the parent gas (deuterium), have been measured using recently identified spectra[15] and a 3-metre normal incidence vacuum spectrograph equipped with a built-in intensity calibration device[16]. Since the ions appear at different times due to the transient nature of the plasma (see sections 4 and 5), and since both these observations and photoelectric observations[17] of Doppler widths indicated a variation with time, two trace elements were added simultaneously and measurements made for ions which appear at the same time. The ratio of observed kinetic

energies for a number of pairs of ions are shown in Table I together with the theoretical ratios expected from equations (23) to (26). The observed ratios fall systematically between those expected from a thermal distribution (equation (23)) and a mass motion (equation (26)). By using three trace elements (Ne, A and Kr) to the discharge, the form of the ion energy distribution was established to be

$$W_i = W_o + w_o M_i/M_D \qquad (27)$$

where W_o = 102 eV and w_o = 2.3 eV in the particular condition investigated and M_D is the mass of the deuteron. The mass motion term is interpreted as being due to a low frequency oscillation perpendicular to the magnetic field (equation (26)) and the constant term is interpreted as a thermal component which is a result of thermalization of the directed mode.

4. Transient Spectra

So far we have only considered steady state systems. However, high temperature laboratory plasmas are usually short-lived and transient effects can be important and have received some detailed studies[18, 19]. For a fully confined plasma in the coronal domain, the steady state ionization equations are replaced by the differential equations describing the rates -

$$\frac{1}{n_e}\frac{dx_i}{dt} = x_{i-1} S_{i-1} - x_i (S_i + \alpha_i) + x_{i+1}\alpha_{i+1} \qquad (28)$$

where x_i is the relative population of the i th state of ionization at time t. For the simple case of a trace element in a fully ionized hydrogen plasma at constant temperature T_e, approximate analytical solutions of (28) are

$$x_i = \beta_i e^{-n_e S_i' t} - \beta_{i-1} e^{-n_e S_{i-1}' t} + \gamma_i \qquad (29)$$

where $S_i' = S_i + \alpha_i + \alpha_{i+1}$ and $\beta_i = 1 - \sum_{o}^{i} \gamma_i$

and γ_i is the steady state value of x_i obtainable from equation (5) and $\sum_{o}^{Z} \gamma_i = 1$.

It is important to differentiate between transient spectra and variable spectra. The former indicate the attempt of the system to reach a steady state whereas the

latter reflect changes in the system e.g. a variation in temperature. When transient effects can be neglected i.e. when the time for ionization equilibrium is short compared to the characteristic time of change of the plasma or its life-time, steady state solutions can be used and changes in n_e or T_e imposed to investigate variable spectra. When both transient and variable effects are present, the analysis of the spectrum is complicated, as is shown by the detailed investigation of the Zeta spectrum by HOBBS et al[20].

5. Partial Containment

So far we have dealt with fully contained plasmas in which the inherent assumption has been that the total number of particles within the system is conserved. However, this is generally not the case for high temperature laboratory plasmas, great difficulty being experienced in producing good confinement systems.

An analysis of the effect of partial containment on transient spectra has been carried out by BURTON and WILSON[19] who introduced a plasma loss rate ($-x_i\lambda$) and an injection rate ($+\Lambda$) of neutrals or lowly ionized ions into the differential equations (28). In this case, x_i and Λ are normalised with respect to the initial number density n_o of the trace element and approximate analytical solutions are

$$x_i = e^{-\lambda t}\left[\beta_i\left(1 - \frac{\Lambda}{n_o\Lambda S_i'/\lambda+\lambda}\right)\exp\left\{-\frac{n_oS_i'}{\lambda}(1-\frac{\Lambda}{\lambda})(1-e^{-\lambda t}) - \frac{\Lambda}{\lambda}n_oS_i't\right\}\right.$$
$$\left. - \beta_{i-1}\left(1 - \frac{\Lambda}{n_o\Lambda S_{i-1}'/\lambda+\lambda}\right)\exp\left\{-\frac{n_oS_{i-1}'}{\lambda}(1-\frac{\Lambda}{\lambda})(1-e^{-\lambda t}) - \frac{\Lambda}{\lambda}n_oS_{i-1}'t\right\} + \gamma_i\right]$$
$$+ \Lambda\left[\frac{\beta_i}{n_o\Lambda S_i'/\lambda+\lambda} - \frac{\beta_{i-1}}{n_o\Lambda S_{i-1}'/\lambda+\lambda} + \frac{\gamma_i}{\lambda}\right] \qquad (30)$$

The variation of ionization population and hence spectral line intensity with time can be divided into two parts, as in the fully confined case; an initial transient followed by a steady state, but the latter is a dynamic steady state due to the balance of injection and loss processes i.e. we have a sustained plasma instead of a contained plasma. Equation (30) reduces to equation (29) in the limit when λ and Λ tend to zero. In this case the observable parameters Δt_i (the average time of duration of the initial

transient) and R_i (the intensity ratio of the steady state to the peak of the initial transient) depend on atomic processes only, whereas they are dominated by the loss and injection rates when these become large. In the fully confined case, Δt_i increases rapidly with i until it becomes infinite for an ion which is heavily populated in the steady state. The presence of a loss rate places a ceiling on Δt_i which is reached when $\lambda \gg n_e S_i$ and is independent of n_e and T_e and given approximately by

$$\text{Limit}_{i \to Z} \; \Delta t_i \to \left(1 + \frac{\Lambda}{\lambda}\right)\frac{e}{2\lambda} \qquad (31)$$

In these conditions, a steady state can only be maintained by an injection of atoms and the intensity ratio R_i is given approximately by

$$R_i = \Delta t_i \Lambda \frac{12(\Lambda/\lambda)^2}{2 + 5\Lambda/\lambda + 5(\Lambda/\lambda)^2} \qquad (32)$$

Using observed values of Δt_i and R_i, equations (31) and (32) can be solved for Λ and λ without knowledge of the electron temperature or the cross sections of the ionization and recombination processes.

This method has been used to investigate plasma containment in Zeta[19, 21]. The effect of a loss rate on the transient form of the spectra is illustrated by Fig. 3 which shows the temporal variation of the intensities of spectral lines due to AI to AVIII inclusive. Also shown, at top and bottom, is the gas current wave-form for the particular Zeta discharge investigated. It will be noticed that the transient life-time Δt_i reaches a ceiling of about 0.3 m sec at AVI and remains constant through AVIII, thus confirming equation (31). For this particular plasma $n_e \sim 10^{14}$ cm^{-3} and $kT_e \sim 20$eV and thus the fully contained case (equation (29)) predicts values of Δt_i which increase rapidly to a value of 33m sec for AVIII. The absence of a tail in the spectral line transients shown in Fig. 3 indicates that there is negligible injection of argon into the discharge.

6. Conclusion

A brief survey has been made of some of the advances made in understanding the basic physics involved in the spectroscopic study of non-thermal plasmas. The form of electron population distribution has been sketched and the domains where simple approximations apply have been defined. Some simple forms of ion energy distribution have been discussed and the general method of investigating these outlined. Also, the effects of transient conditions and plasma loss processes on the observed spectra have been indicated. There are still many outstanding problems, in particular, the effect of radiation trapping on the electron population distributions, together with several instrumental problems associated with spectroscopic work in the vacuum ultraviolet and soft X-ray regions of the spectrum.

7. Acknowledgements

The survey presented above is largely based on the work of the Plasma Spectroscopy Group at the Culham Laboratory and I am indebted to several colleagues for advice and criticism, in particular to Dr. R.W.P. McWhirter, Mr. W.M. Burton, Dr. A.G. Hearn and Mr. B.B. Jones. My thanks are also due to Mr. R.S. Pease for several critical discussions.

References:

1. G. JÜRGENS, Z. Physik, 134, 21, (1952).
2. E.A. McLEAN, C.E. FANEUFF, A.C. KOLB and H.R. GRIEM, Phys. Fluids, 3, 843 (1960).
3. L. SPITZER, JR, Physics of Fully Ionized Gases, Interscience, N.Y. (1956)
4. R.V.D.R. WOOLLEY and C.W. ALLEN, Mon. Not. Roy. Astr. Soc., 108, 292 (1948).
5. R.W.P. McWHIRTER, Nature, 190, 902 (1961).
6. D.R. BATES and A.E. KINGSTON, Nature, 189, 652 (1961).
7. D.R. BATES, A.E. KINGSTON and R.W.P. McWHIRTER, Proc. Roy. Soc., in press (1962).
8. N. D'ANGELO, Phys. Rev., 121, 505 (1961).
9. R.W.P. McWHIRTER, private communication (1962).
10. M.J. SEATON, Atomic and Molecular Processes (Ed. Bates) Academic Press, N.Y. (1962).
11. H.A. BETHE and E.E. SALPETER, Handbuck der Physik, 35, 88 (1957).
12. G. ELWERT, Zeit F. Natur., 7a, 432 (1952).
13. P.C. THONEMANN, Optical Spectrometric Measurements of High Temperatures (Ed. Dickerman), Un. Chicago Press (1961).
14. B.B. JONES and R. WILSON, I.A.E.A. Conf., Salzburg CN-10/57, (1961).
15. B.C. FAWCETT, B.B. JONES and R. WILSON, Proc. Phys. Soc., 78, 1223 (1961).
16. B.B. JONES, Applied Optics, 1, May (1962).
17. A.G. HEARN, B.B. JONES and S.A. RAMSDEN, J. Nuc. Energy Pt. C, 4, 23 (1962).
18. R.W.P. McWHIRTER, W.G. GRIFFIN and T.J.L. JONES, 4th Conf. Ionization Phenomena, Uppsala, 833 (1959).
19. W.M. BURTON and R. WILSON, Proc. Phys. Soc. 78, 1416, (1961).
20. G.D. HOBBS, R.W.P. McWHIRTER, W.G. GRIFFIN and T.J.L. JONES, 5th Conf. Ionization Phenomena, Munich, (1961).
21. R.S. PEASE et al, I.A.E.A. Conf. Salzburg, CN-10/60, (1961).

TABLE I

Observed ratios of ion energies compared with theoretical ratios for different forms of heating

Energy Ratio	Z^2/M	Thermal	M	Observed
$\frac{AVIII}{OVI}$	0.8	1.0	2.5	1.3 ± 0.1
$\frac{AVIII}{NeVI}$	1.0	1.0	2.0	1.1 ± 0.1
$\frac{AVII}{NeV}$	1.1	1.0	2.0	1.2 ± 0.1
$\frac{KrVIII}{AVII}$	0.6	1.0	2.1	1.3 ± 0.1
$\frac{KrVIII}{NeV}$	0.7	1.0	4.1	1.6 ± 0.1

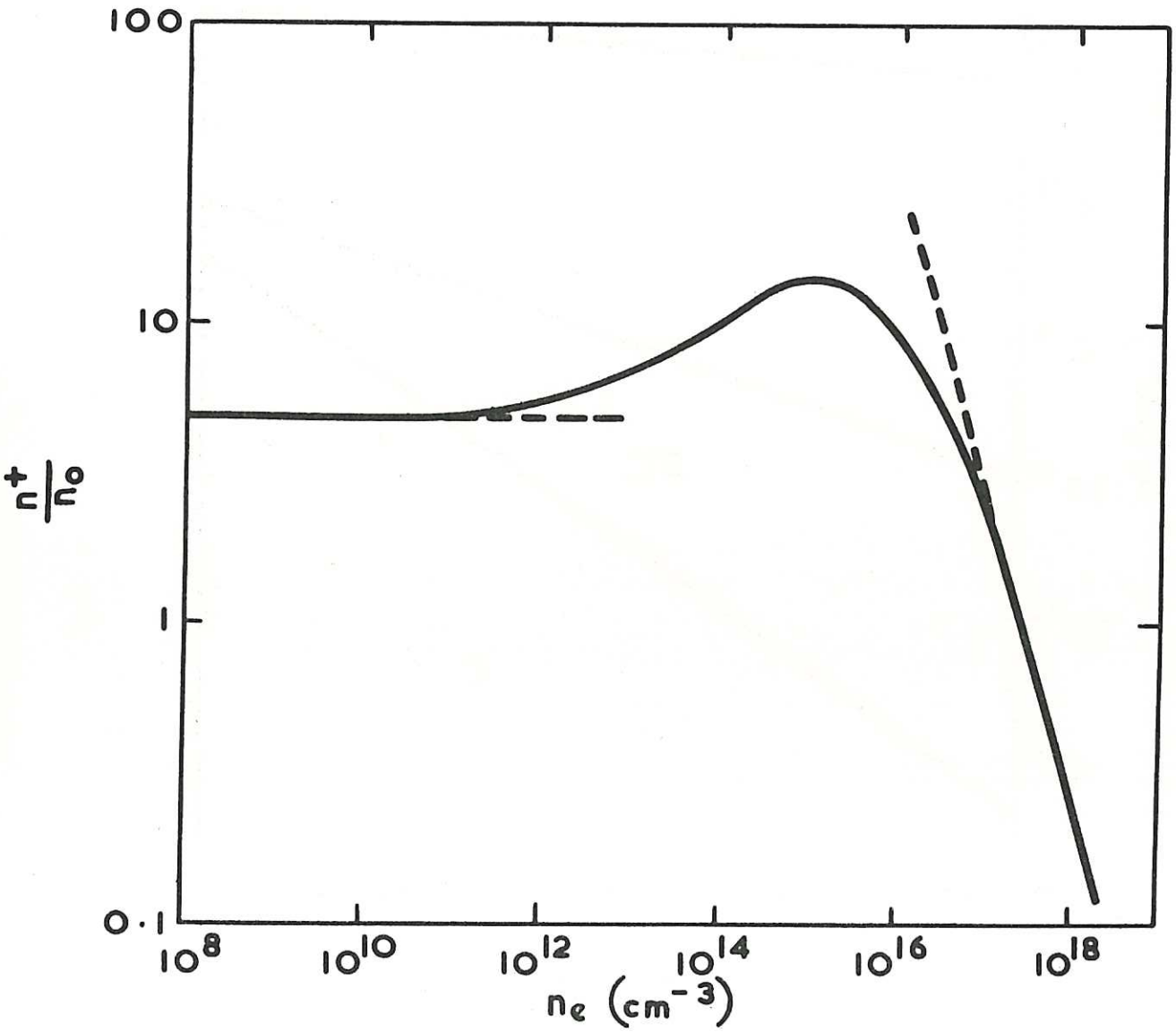

CLM–P9. FIG.1.

Ionization ratio n^+/n_o is a hydrogen plasma at T_e = 16,000°K as a function of electron density n_e from the calculations of BATES et al (7). The dashed lines indicate coronal (independent of n_e) and thermal ($\propto n_e^{-1}$) distributions.

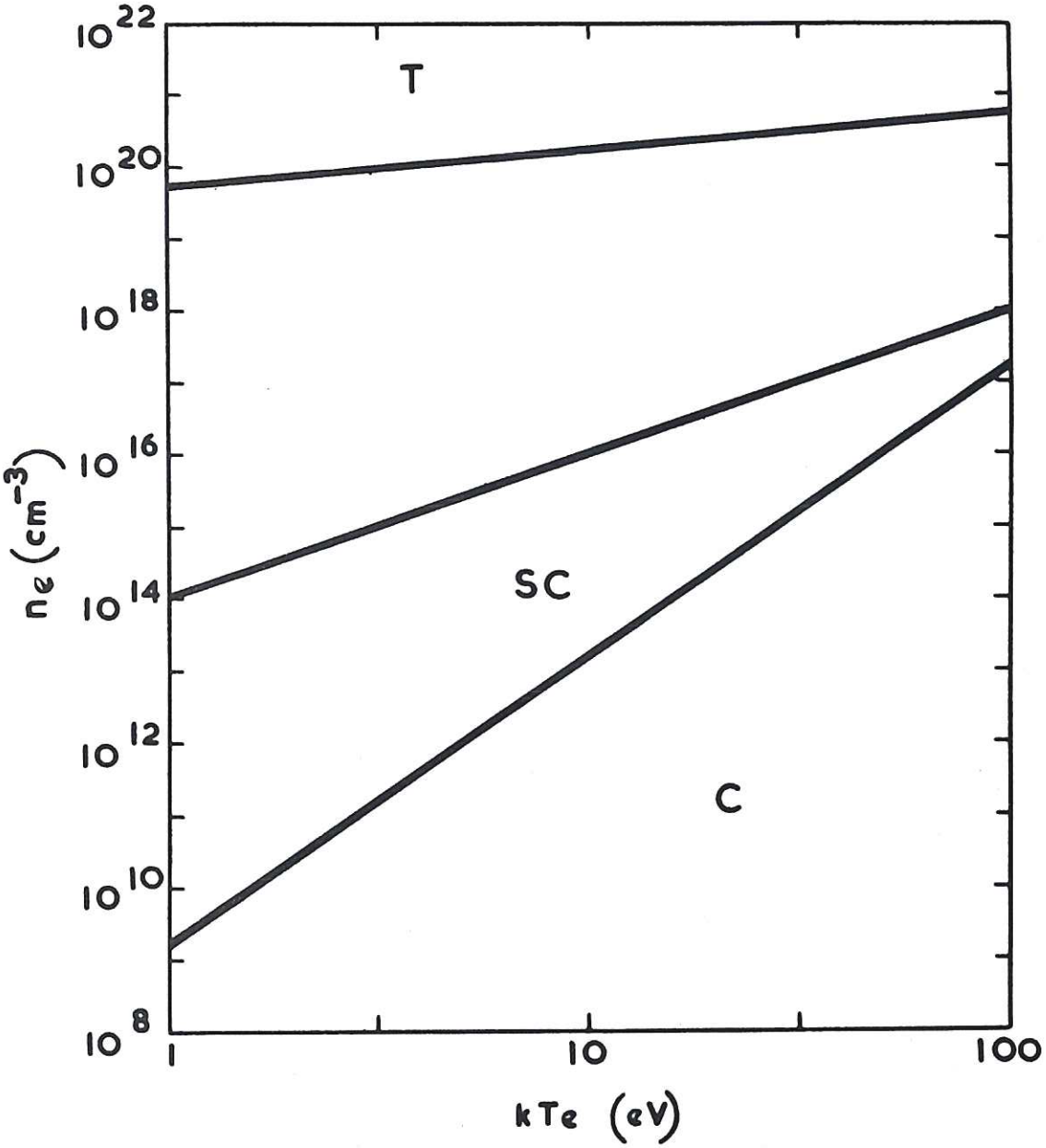

CLM–P9. FIG.2.

Domains of validity for various types of electron distributions for an ion of ionization potential = 100 eV in an optically thin plasma of electron density n_e and electron temperature T_e. T - thermal; C - coronal; SC - Semi-coronal (see text).

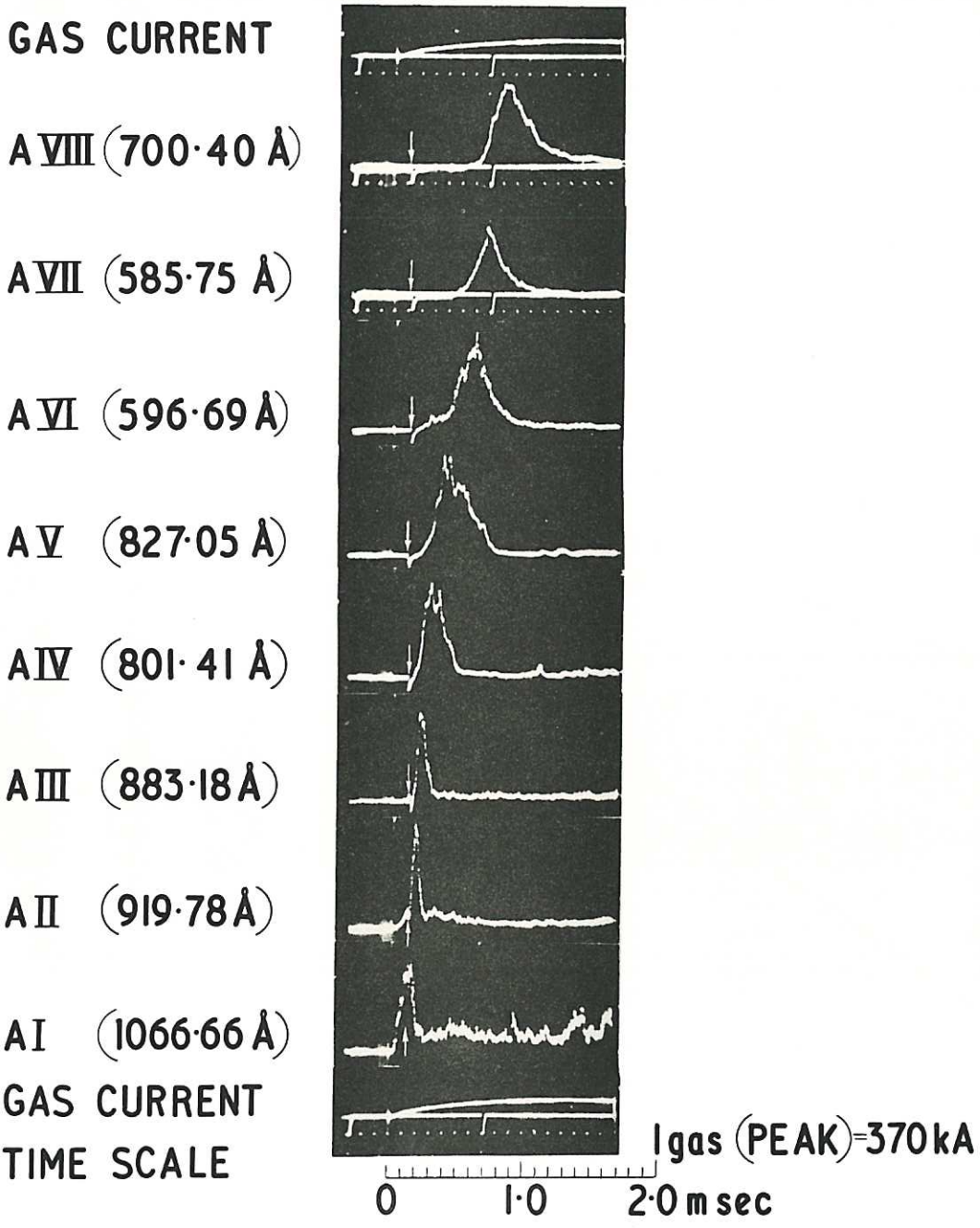

CLM–P9. FIG.3.

Temporal variation of the intensities of specral lines due to AI to AVIII inclusive showing the successive appearance of the ionization states in the Zeta plasma. Note that the life-time of each feature reaches a constant value at about A VI, caused by a loss of plasma from the system. The argon is introduced as a 5 per cent impurity in deuterium with a total gas pressure of 0.5 millitorr.